Comparison Between the Number of Discernible Colors in a Digital Camera and the Human Eye

J. Pujol[a], F. Martínez-Verdú[b], M.J. Luque[c], P. Capilla[c], M. Vilaseca[a]
[a] Center for Development of Sensors, Instrumentation and Systems, Dept. of Optics and Optometry, Technical University of Catalonia Terrassa, Barcelona/Spain
[b] Dept. of Optics, University of Alicante Alicante, Spain
[c] Dept. of Optics, University of Valencia Burjassot, Valencia/Spain

Abstract

Since an input device is not a colorimeter and its opto-electronic behavior is not ideal, its color gamut is smaller than that of the CIE-1931 XYZ standard observer. A chromatic discrimination model and packing algorithm to the color discrimination ellipses have been used to compute the number of distinguishable colors within the frontiers of MacAdam's optimal color loci. We have found that, due to the short dynamic range of the digital camera response, this distinguishes considerably fewer dark colors than light ones, but relatively much more colors with middle lightness (Y between 40 and 80, or L* between 69.5 and 91.7).

Introduction

Successful color management depends on knowing the color gamut and the color profile of the color device used. Determining the gamut of output devices (displays, projectors and printers) is relatively easy, both when colors in display or in paper are generated systematically[1] and when color profiles are applied[2]. However, obtaining this gamut in input devices (scanners and digital cameras) presents more conceptual problems. Displays, projectors and printers are electro-optical devices, that is, they generate digital color images by physical and electronic procedures that are finally seen in a medium (display, screen or paper), with a one-to-one correspondence between RGB or CMYK digital data triad and a color-stimulus. Scanners and digital cameras are opto-electronic devices[3], that is, they encode the light distribution from the original image by physical and electronic procedures, yielding a digital image that can be displayed with an output device and saved in any image format file. These basic differences are shown schematically in Figure 1.

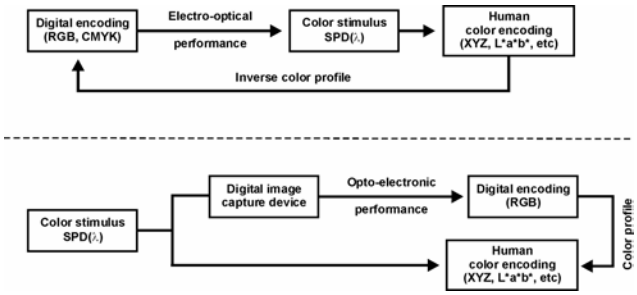

Figure 1: Basic performance of color devices. Top: output devices (displays, projectors and printers). Bottom: input device (scanners and cameras). SPD(λ) is the spectral power distribution or spectrum of the color-stimulus.

The key factor in the performance of input devices is the univariance principle: spectrally different color stimuli may give rise to identical RGB digital data. Therefore, it is very difficult to determine which color-stimulus corresponds to a RGB triad if the captured scene is not previously known. If we capture a reference scene of known colors (for instance, from a color atlas such as Munsell or NCS), and determine the corresponding RGB values, to analyze these the RGB digital data are transformed into XYZ data in order to determine how the input device encodes these color-stimuli in comparison with the human eye. To do this, we must apply the input device color profile to the RGB values to derive the corresponding XYZ values. Note that the gamut of output devices can be obtained far more simply.

To compute the gamut of an input device it is necessary previously to select the color-stimuli of the scene and a characterization model, which must include at least information about the spectral characterization (color-matching functions) and about the colorimetric characterization (opto-electronic conversion functions).

Recently, two works[4,5] approaching this subject with slightly different methods have been published. In our work[5] the gamut of a digital camera, in raw performance (i.e. without color correction), is derived from the simulation of the capture of the optimal or MacAdam[6,7] color-stimuli, concluding that the device gamut is smaller than that of the colorimetric standard observer (Fig. 2).

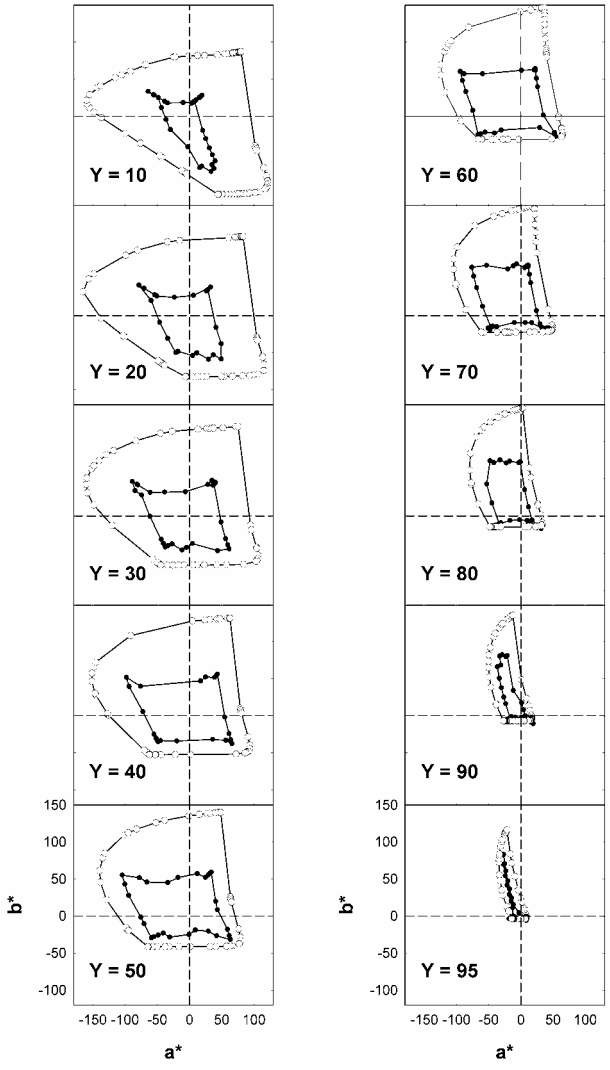

Figure 2: MacAdam limits with different luminance factors in the CIE-(a,b*) diagram, for the CIE-XYZ standard observer (outer line with hollow symbols) and for a digital camera (inner lines with solid symbols).*

Using these data, an algorithm calculating the number of discernible colours of an input device and of the human eye (CIE-XYZ standard observer) is proposed, assuming that both have the same colour metric. A priori, this is achieved estimating the number of the discrimination ellipsoids filling the color solid, which in the human case is associated to the MacAdam limits or Rösch color solid[6,7]. This estimation is usually approximated by fixating the luminance factor Y or the lightness L*, so the computation of discrimination ellipsoids becomes the computation of the discrimination ellipses plus an interpolation of the just-noticeable lightness differences between a fixed value and the next one[8,9]. The sources of the experimental data about discrimination ellipses there are numerous[10-15]. We have chosen the Krauskopf and Gegenfurtner data[14,15] because they allow the homogeneous sampling of the color solid.

Methodology and results

From our previous work[5], we have obtained the data of the MacAdam limits under an equal-energy illuminant, for different luminance factors Y, of an input device (Sony DXC-930P camera) and the CIE-XYZ standard observer (Fig. 2). The initial conditions of the simulated capture of the optimal or MacAdam color-stimuli are: illuminance level E = 1000 lx, white balance adjusted to 5600 K (offset value), f-number of the zoom lens equal to 4 and photosite integration time equal to 20 ms.

The computation of the distinguishable colors by the human eye implies some assumptions and complications when our objective is to determine the total number of discrimination ellipsoids inside the Rösch color solid. The same difficulties appear if an input device is considered, always assuming that this color device has the same color metric as the human eye. We do not discuss this topic and we concentrate ourselves in the estimation of the percent reduction of the discernible colors by our camera relative to the human eye. Therefore, we estimate the number of discrimination ellipses within the MacAdam limits for different luminance factors, both with the CIE standard observer and with our digital camera, and then compare them. In this way, we may obtain additional information about the limitations of the digital camera as an opto-electronic additive color device. Therefore, we aim only to show a method that can be applied to any input device (scanner and digital camera).

The discrimination ellipses have been computed with a discrimination model derived from the experimental data of Krauskopf and Gegenfurtner[14,15], which is based on the MacLeod-Boynton color space[16], although with a different scaling condition. In this color space, colors in the same vertical line in the chromatic diagram have constant L and M values, while colors in the same horizontal line have constant values of S and $(L+M)$ (see Figure 3 bottom). Accordingly, a vertical line contains colors that would give constant response in a red-green mechanism, $T = L - \alpha M$, no matter the value of α. Analogously, a horizontal line contains colors yielding constant response in a yellow-blue mechanism of the type $D = S - \beta(L+M)$, no matter the value of β. In particular, those colors in the $D = 0$ and $T = 0$ lines elicit response only from the T or the D mechanism, respectively, and are therefore the cardinal directions of T and D.

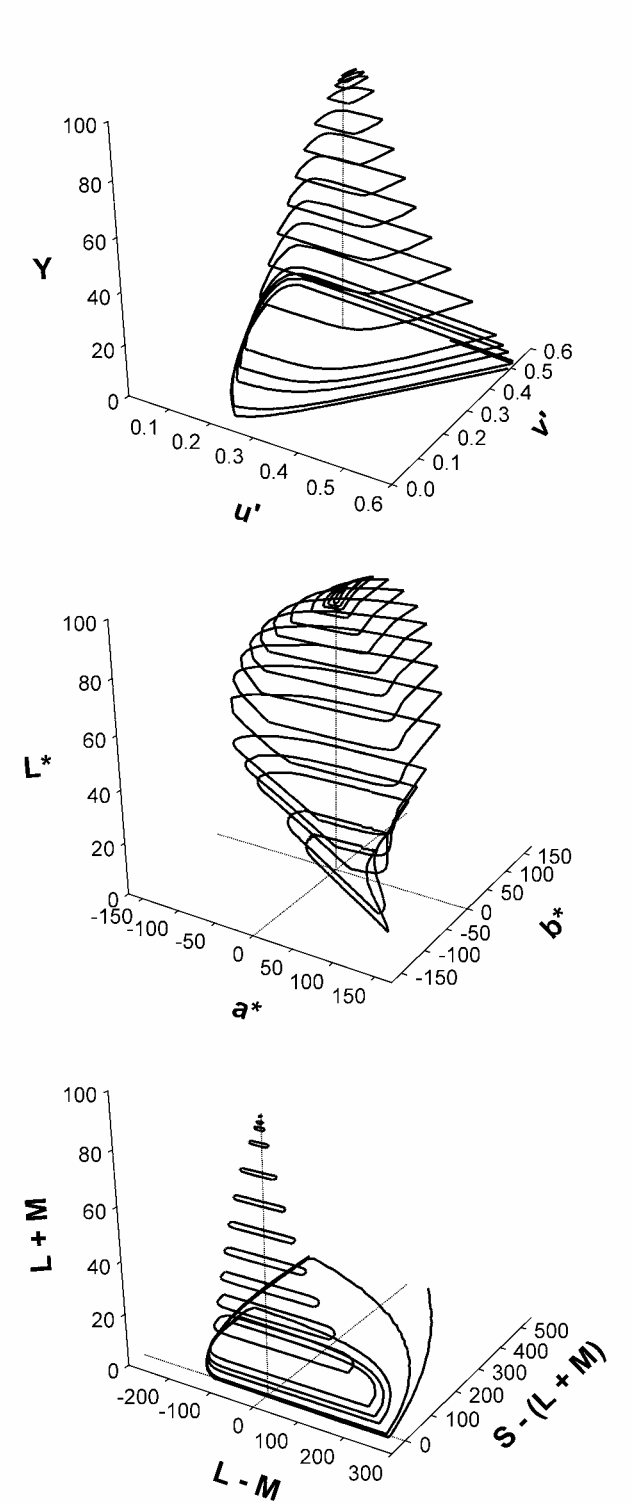

*Figure 3: Rösch color solid with equal-energy illuminant in the color spaces CIE-u'v'Y (top), CIE-L*a*b* (center) and MacLeod-Boynton scaled by Krauskopf-Gegenfurtner (bottom). The data base consists of 1734 optimal colors grouped by its luminance factor Y ={1,2,5,7,10,20,30, 40,50,60,70,80,90,95,97,99}.*

In this color space, discrimination ellipses are computed as follows. The discrimination ellipse around the equal-energy white (T = 0, D = 0) defines the unity threshold in each cardinal direction. Thus, in these unities the discrimination ellipse around (T = 0, D = 0) is a circle of unity radius. Let us consider a pedestal in the T cardinal direction. Thresholds along this direction are proportional to the T response to the pedestal, whereas thresholds along the orthogonal D direction are constant. Analogously, if the pedestal is on cardinal direction D, thresholds along the D direction are proportional to the D response to the pedestal, whereas they are constant along the orthogonal T direction. In consequence, discrimination ellipses around stimuli in one of the cardinal directions are oriented along that direction. The rate at which the major axis of each ellipse changes along each cardinal direction was taken from the experimental data of Krauskopf and Gegenfurtner. When the pedestal is not on one of the cardinal directions, the laws governing thresholds are not so simple. Discrimination ellipses around a pedestal in the first or third quadrant of the modified MacLeod-Boynton space seem to be oriented along the cardinal directions. The sizes of the major and minor axis of the ellipses are proportional to the T or D responses elicited by the pedestal. This result can be explained if we admit the existence of two independent discrimination mechanisms, whose cardinal directions are the T and D directions of MacLeod-Boynton's diagram, and that interact vectorially. However, discrimination ellipses around pedestals in the second or fourth quadrant seem to be oriented along the direction defined by the pedestal. This result seems to imply the existence of a continuum of mechanisms syntonized along equally spaced directions in the color space. The directions along which are syntonized these hypothetical mechanisms could be deduced approximately from the experimental data, but the threshold increment rate along each of these directions cannot. Although it could reasonably be admitted that thresholds again would increase with increasing distance to the white stimulus, the actual law of variation would be still to be determined. Because our aim is to compare the number of ellipses within the MacAdan limits in the human observer and the camera, and not to reach the best estimation of this number, the model of two cardinal directions is enough. To avoid further complications, we will assume that the variation laws of thresholds are independent from luminance.

The next problem to solve is which method to use to pack the discrimination ellipses. We have followed two different procedures. With what we call the *tangent criterion*, we determine the position of the centers of the ellipses to verify two conditions: 1) each ellipse is tangent to other four at its vertices and 2) the centers of two adjacent ellipses have either the same T or the same D value. This criterion does not yield optimal packing, because the gaps between ellipses increase with the distance to the achromatic point[17,18]. The second strategy, that we call *dense packing*, consists in placing the centers of the ellipses on the centers of the tiles of an hexagonal mosaic covering the space to which we have applied a non-linear

transform [x*f(x), y*f(y)]. The functions f(x) and f(y) have been found empirically, and verify that the overlap between ellipses is small. In this way we come nearer to an optimum ellipse packing. The results obtained for the human eye and our camera for Y = 40 % and the dense criterion are shown as an example in Figure 4.

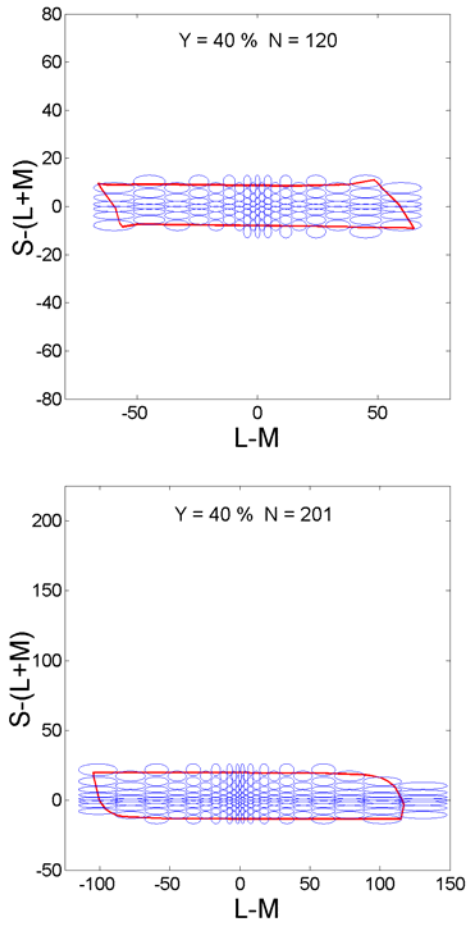

Figure 4: Dense packing of the discrimination ellipses inside the MacAdam limits for the luminance factor Y = 40 % (L = 69.5) for the input device (top) and for the human eye (bottom). N is the number of the discernible colors or discrimination ellipses inside each locus.*

The two packing criteria produce basically the same results, as can be seen in Figure 5, where we have plotted the number of distinguishable colors versus the luminance factor, both for the human eye and our camera. Surprisingly, in the range of luminance factors explored, which goes as low as 1%, the curve obtained for the camera has an optimum (around 20%), whereas the curve for the human observer hasn't. We would expect that the number of distinguishable colors for the standard observed would decrease as the luminance factor approaches to zero (ideal black). With the discrimination model used, the number of ellipses would increase indefinitely as the luminance factor decreases. Let us remember, however, that our model did not include the influence of the adapting luminance on discrimination thresholds. Therefore, we cannot predict correctly the luminance factor below which the number of distinguishable colors decreases.

Figure 6 shows also some interesting features. Here we show the change in the number of colors than can be distinguished by the camera (with N = 4 and t = 20 ms), as a function of the luminance factor, but relative to the standard colorimetric observer. In the middle range of Y values, the relative reduction factor is approximately constant. That is, with this exposure value, the camera the reduction in the number of distinguishable colors is greater for dark than for light colors, and this reduction is minimal for colors with intermediate lightness (Y between 40 and 80, or L* between 69.5 and 91.7). The gap between Y = 97 % and Y = 99 % is due to the fact that when Y tends to 100%, both for the camera and the human eye the number of distinguishable colors tends to one (the perceptual or equal-energy white).

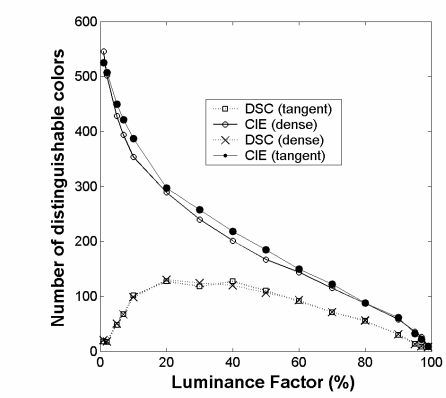

Figure 5: Number of discernible colors according to the luminance factor and ellipses packing method in the input device and the human eye.

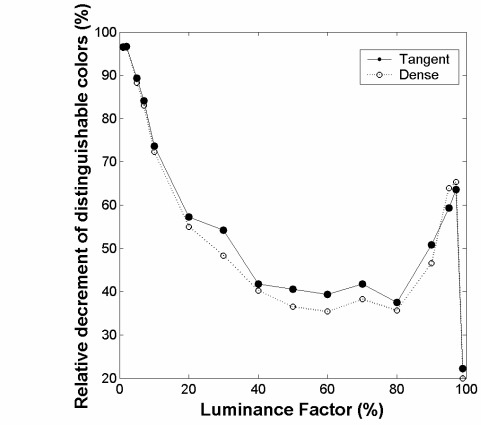

Figure 6: Relative decrement of discernible colors according to the luminance factor in the input device respect to human eye.

Conclusions

The method proposed serves to compare the performance of any opto-electronic input device with that of the standard colorimetric observer, taking as the comparison criterion the number of distinguishable colors within the frontiers of MacAdam optimal-color loci. For the particular camera we have used, we have found maximal reduction of distinguishable colors for both the highest and lowest luminance factor. This happens because the dynamic range of the digital camera is shorter than that of the human eye: very dark and light colors belong to the regions near the regions where noise and saturation impair performance, respectively.

Acknowledgements

This research was supported by the Ministerio de Ciencia y Tecnología (Spain) under grant DPI2002-00118. M. Vilaseca would like to thank the Generalitat de Catalunya for the PhD grant she has received. We wish also to thank to Prof. J.L. Monterde García-Pozuelo, member of the Department of Geometry and Topology of the University of Valencia, for valuable advice on packing algorithms with ellipses.

References

1. J. Morovic, P.L. Sun, How different are colour gamuts in cross-media colour reproduction?, in Colour Image Science, John Wiley & Sons, Chichester, 2002, pg. 237.
2. M. Mahy. Colour gamut determination,. in Colour Engineering, John Wiley & Sons, Chichester, 2002, pg. 263.
3. B.A. Wandell, D.L. Silverstein. Digital Color Reproduction, in The Science of Color, 2nd ed., Elsevier, New York, 2003, pg. 281.
4. J. Morovic, P. Morovic. Color Res. Appl., 28, 59 (2003).
5. J. Pujol, F. Martínez-Verdú, P. Capilla, Estimation of the Device Gamut of a Digital Camera in Raw Performance using Optimal Color-Stimuli, Proc. PICS, pg. 530 (2003).
6. G. Wyszecki, W.S. Stiles, Color Science: Concepts and Methods, Quantitative Data and Formulae, 2nd ed., John Wiley & Sons, New York, 1982, pg. 179.
7. R.S. Berns, Billmeyer and Saltzman's Principles of Color Technology, 3rd ed., John Wiley & Sons, 2003, pg. 62, 143.
8. M.R. Pointer, G.G. Attridge, Color Res. Appl., 23, 52 (1998).
9. R.G. Kuehni, Color Space and Its Divisions: Color Order from Antiquity to the Present, John Wiley & Sons, New York, 2003, pg. 202.
10. D.L. MacAdam, J. Opt. Soc. Am., 32, 247 (1942).
11. W.R.J. Brown, D.L. MacAdam, J. Opt. Soc. Am., 39, 808 (1949).
12. G. Wyszecki, G.H. Fielder, J. Opt. Soc. Am., 61, 1135 (1971).
13. J. Romero, J.A. García, L. Jiménez del Barco, E. Hita, J. Opt. Soc. Am. A, 10, 827 (1993).
14. J. Krauskopf, K.R. Gegenfurtner, Vis. Res., 32, 2165 (1992).
15. J. Krauskopf. Higher order color mechanisms, in Color Vision: From Genes to Perception, Cambridge University Press, Cambridge, 1999, pg. 310.
16. D.L. MacLeod, R.M. Boynton, J. Opt. Soc. Am., 69, 1183 (1979).
17. R.S. Berns, Billmeyer and Saltzman's Principles of Color Technology, 3rd ed., John Wiley & Sons, 2003, pg. 115.
18. M.R. Luo, G. Cui, B. Rigg, Color Res. Appl., 26, 340 (2001).

Biography

Jaume Pujol received his BS in Physics form the University Autonoma of Barcelona in 1981 a Ph.D. in Physics from the same University in 1990. Since 1984 he teaches Vision and Color Sciences at School of Optics & Optometry in the Technical University of Catalonia (Spain). His work is primarily focused on Color Imaging (device calibration and characterization, color management), Industrial Colorimetry and Optics of the Human Vision. He is a member of ARVO, OSA, IS&T and the Spanish Optics Society (SEDO). E-mail: pujol@oo.upc.es.